Original Article

Protective effects of muscone on traumatic spinal cord injury in rats

Chao Yu[1], Fei Gui[1], Qian Huang[2], Yuanmeng Luo[1], Zili Zeng[1], Ruifu Li[1], Liang Guo[1]

[1]Department of Orthopedics, University-Town Hospital of Chongqing Medical University, Chongqing, China; [2]Department of Orthopedics, The 1st Affiliated Hospital of Chongqing Medical University, Chongqing, China

Contributions: (I) Conception and design: L Guo; (II) Administrative support: C Yu; (III) Provision of study materials or patients: C Yu, Q Huang, F Gui; (IV) Collection and assembly of data: Y Luo, Z Zeng; (V) Data analysis and interpretation: R Li; (VI) Manuscript writing: All authors; (VII) Final approval of manuscript: All authors.

Correspondence to: Liang Guo. Department of Orthopedics, University-Town Hospital of Chongqing Medical University, 55 university town middle Road, Shapingba District, Chongqing 401331, China. Email: guoliang@hospital.cqmu.edu.cn; 462986302@qq.com.

Background: Traumatic spinal cord injury (SCI) is a major clinical concern, and it is a life-changing neurological condition with substantial socioeconomic implications. Muscone has been widely used in traditional Chinese medicinal formulations for its anti-inflammatory activity. However, its protective effects on traumatic SCI have not been explored. This study investigated whether muscone plays a protective role in SCI and compared its effects with those of methylprednisolone sodium succinate (MPSS).

Methods: Rats were divided into five groups: normal saline (NS; n=24), methylprednisolone (MP; w=24), and muscone 1 (MO1), muscone 2 (MO2), and muscone 3 (MO3) (n=24 in each group, collectively called the MOx groups). The SCI rat model was established by the modified Allen's method. The rats were administered muscone (MO1: 2.5 mg/kg, MO2: 5 mg/kg, and MO3: 10 mg/kg) or MP (30 mg/kg), or an equivalent volume of saline. The rats were kept under observation for 4 weeks. Malondialdehyde (MDA), superoxide dismutase (SOD), interleukin-6 (IL-6), interleukin-1β (IL-1β), and tumor necrosis factor-alpha (TNF-α) levels were detected using enzyme-linked immunosorbent assay (ELISA). The expression of glial fibrillary acidic protein (GFAP), B-cell lymphoma-2 (BCL-2), and caspase3 was detected by western blot analysis. Hematoxylin-eosin (HE), Nissl, and immunocytochemistry (ICC) staining was performed for pathological observation. Basso-Beattie-Bresnahan motor function scores were evaluated for assessment of neural functions after acute SCI.

Results: Muscone inhibited immune-inflammatory reactions, neuronal necrosis, and apoptosis. The lower limb function recovery was better in the MOx groups compared with NS and MP groups according to Basso-Beattie-Bresnahan scores. The changes were remarkable in the MO2 group compared with the other groups.

Conclusions: Muscone alleviates secondary injury after SCI by reducing immune-inflammatory reactions, neuronal necrosis, and apoptosis.

Keywords: Anti-inflammatory agents; astrocytes; glial fibrillary acidic protein (GFAP); spinal cord injury (SCI)

Submitted Apr 19, 2022. Accepted for publication Jun 20, 2022.
doi: 10.21037/atm-22-2672
View this article at: https://dx.doi.org/10.21037/atm-22-2672

Introduction

Traumatic spinal cord injury (SCI) is one of the major health challenges worldwide, with an estimated incidence of 56.4 per 1,000,000 traumatic injuries in the US in 2019 (1); it has devastating physical, psychosocial, and vocational implications for patients and caregivers (2-4). SCI can be

categorized into primary and secondary phases (5-7). A cascade of secondary injury destroys an increasing zone of tissue adjacent to the primary injury site and exacerbates neurological deficits and outcomes (8-11), such as cellular excitotoxicity, ionic dysregulation, disruption of the blood-spinal cord barrier, free-radical-mediated peroxidation, and immune-inflammatory reactions, which are considered pathological damage-mediating processes during secondary damage (12-15). Inflammatory cytokines are considered the key regulating substances during immune reactions, which participate in adjusting inflammatory responses in SCI (16-18). Methylprednisolone sodium succinate (MPSS) can be considered within 8 hours after injury for patients without significant medical contraindications. It upregulates the release of anti-inflammatory cytokines and reduces oxidative stress to enhance neural cell survival in preclinical models of traumatic SCI (2), but it is limited by its major systemic adverse effects (19).

Muscone (20), one of the macrocyclic musk compounds, has been widely used in traditional Chinese medicinal formulations. Muscone can also be synthesized. It has pharmacological effects, including promoting blood circulation and menstruation, inducing resuscitation, and exerting anti-inflammatory activity (21-26). It is widely used in the treatment of dementia, cerebral ischemia, myocardial infarction, diabetic peripheral neuropathy, vertebral end-plate degeneration, injury, inflammation, cancer, and other diseases (27-38). Muscone is one of the anti-inflammatory constituents in a well-known traditional Chinese medicine named Pian-Tze Huang (39). It can reach various parts of the central nervous system through the blood–brain barrier within 5 minutes after gastric administration and within 2 minutes after caudal vein injection (40). Yu *et al.* verified that muscone exerted potent neuroprotective activity against glutamate-stimulated oxidative stress and Ca^{2+} overload (27).

However, the protective effects of muscone on traumatic SCI have not been explored. This study explored whether muscone plays a protective role in SCI and compared its effects with those of MPSS. We present the following article in accordance with the ARRIVE reporting checklist (available at https://atm.amegroups.com/article/view/10.21037/atm-22-2672/rc).

Methods

Animal grouping and administration

Animal experiments were performed under a project license granted by the Ethics Review Board of the University-Town Hospital of Chongqing Medical University (No. LL-202133), in compliance with national guidelines for the care and use of animals. A protocol was prepared before the study without registration. This study was performed on 120 healthy adult female Sprague-Dawley (SD) rats, each weighing 250–300 g, obtained from the Experimental Animal Center of Chongqing Medical University. Rats were fed in a clean and closed environment in the experimental animal center, with a constant temperature of 20–25 degrees and air humidity of 50%. There were 5 rats in each cage. The rats were equally and stochastically divided into five groups: normal saline (NS), methylprednisolone (MP), and three groups treated with muscone (MO1, MO2, and MO3, collectively called the MO_x groups). Further, 2.5, 5, and 10 mg/kg muscone was injected into the caudal vein immediately after the surgery in the MO_x groups, as follows: MO1, 2.5 mg/kg; MO2, 5 mg/kg; and MO3, 10 mg/kg, and continued for 7 days. Also, 30 mg/kg MPSS was injected into the caudal vein immediately after the surgery in the MP group. An equal amount of NS was injected immediately after the surgery in the NS group. Ten rats died after operation, including 6 rats in Group MP and 4 rats in Group MO3, and 10 rats were finally supplemented.

Anesthesia and surgical procedures

For anesthesia, 4% chloral hydrate at a dose of 0.35 mL/kg was injected into the caudal vein of all rats. They were immobilized in the ventricumbent position. The dorsum of these rats was barbered. Iodophor was used to disinfect the processus spinosus of the eighth thoracic vertebra (T8) in the center before surgery. A posterior median incision was chosen, and lamina and processus spinosus of T7–9 were displayed and removed. The medulla spinalis of the T8 level was hit by using the modified Allen's method. A hammer of 5 mm diameter and 10 g mass was allowed to fall freely on the medulla spinalis from a height of 2.5 cm. It vertically struck the soft and concave plastic sheet, which directly contacted the spinal dura mater and permitted the transfer of static energy to the medulla spinalis of the T8 level (*Figures 1*,*2*). Soft tissues, such as muscle and derma, were seamed in successive layers after a successful strike.

Sign of successful strike

The shrinkage of legs, spastic tail swing, and torso-like flutter were noticed when the medulla spinalis of the T8 level was hit. The lower extremities showed no activities and

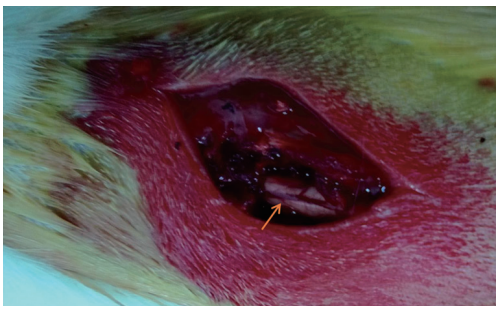

Figure 1 Before spinal cord injury at T8 level of rats. The arrow marks the normal spinal cord tissue.

Figure 2 After spinal cord injury at T8 level of rats. The arrow marks the local bleeding and swelling of the injured spinal cord tissue.

flaccid paralysis, indicating that the model was successful. Penicillin (1.0×10^5 IU/day) was administered after the surgery. The rats were raised at an indoor temperature of 20–25 ℃. The bladder was extruded twice a day (8:00 am and 8:00 pm) before the recovery of spontaneous urination.

Specimen collection

Six rats were randomly chosen from each group on postoperative days 1, 3, 7, and 14. They were fixed in the dorsal position after intraperitoneal anesthesia. The thoracic cavity was opened to expose heart in the field of vision. A syringe needle was inserted into the ascending aorta through the left ventricle, and the right auricle was opened. Further, 200 mL of saline, including 10 U/mL heparin, was rapidly perfused until the fluid was clear. Then, 200 mL of 2% glutaraldehyde was slowly perfused at 4 ℃ until the extremities and tail were hardened. A section of medulla spinalis of T8 was completely excised according to the original incision and fixed with 4% paraformaldehyde for 2 days.

Three rats in each group were randomly chosen at 3 and 8 h, 1 and 3 days, and 1 and 2 weeks after the surgery. After intraperitoneal anesthesia with 4% chloral hydrate at a dose of 0.35 mL/kg, 1 mL of blood was drawn with a capillary glass tube outside the canthus, placed for 2 hours at 20 ℃, and then into a water bath at 37 ℃ for 30 minutes of incubation, and centrifuged at 1,500 rpm for 15 minutes. The supernatant was absorbed into a 1 mL PV tube with 200 μL attractor, and immediately placed in a −80 ℃ refrigerator.

Biochemical analyses

All biochemical analyses were performed at the Laboratory of Biochemistry, School of Life Science, Chongqing Medical University. The tissue samples were stored at −80 ℃ and then homogenized in 0.9% NaCl solution using a tissue homogenizer (T25; IKA-GmbH, Labortechnik, Staufen, Germany). The tissue samples in each group ranged from 127 to 190 mg. After homogenization, the samples were centrifuged (5,000 rpm) at 4 ℃ for 30 minutes. The supernatants were used for detecting the following: malonyldialdehyde (MDA), superoxide dismutase (SOD), interleukin (IL)-6, IL-1β, and tumor necrosis factor-alpha (TNF-α), using enzyme-linked immunosorbent assay (ELISA) at different time points according to the manufacturer's instructions.

Histopathological analyses

Injured spinal cord segments were stored in 10% neutral buffered formaldehyde solution and embedded in a paraffin block by a standard method. Each block was cut into 5 μm-thick coronal sections and trimmed with a Leica microtome (Leica RM2035; Leica, Wetzlar, Germany). The sections were stained with hematoxylin-eosin (HE) and examined under a light microscope (Olympus BH-2; Olympus, Tokyo, Japan) by a blinded pathologist. Specimens were photographed (Sony, CCD-IRISI; Sony Inc., Tokyo, Japan), and all sections were evaluated for the presence of hemorrhage, edema, and neutrophilic infiltration.

Neurological function evaluation after SCI

The scores of Basso-Beattie-Bresnahan (BBB) motor functions of all rats were recorded on postoperative days 1, 3, 7, 14, 21, and 28. The recovery of motor functions in all rats was observed by two physicians not involved in modeling.

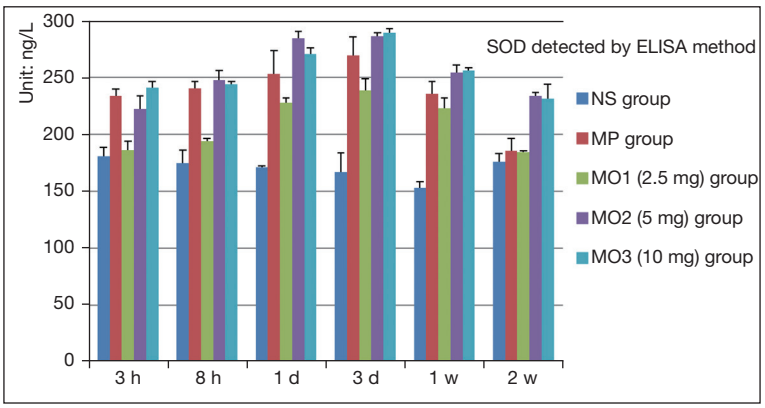

Figure 3 SOD level increased in the MP and MO_x groups compared with the NS group and was the highest in the MO2 group. SOD, superoxide dismutase; MP, methylprednisolone; MO, muscone; NS, normal saline.

Statistical analyses

Data were analyzed using the statistical software SAS V9.4 (SAS Institute, Cary, NC, USA) and presented as mean ± standard deviation(s). The differences between groups were compared using analysis of variance. The pairwise means were compared by the Student-Newman-Keuls (SNK) method. A P value of <0.05 indicated a statistically significant difference.

Results

The traumatic SCI model was established successfully in this study using the modified Allen's method. Spastic tail swing, torso-like flutter, and retraction of lower extremities were noted after hitting the dorsal spinal cord. The lower extremities showed no activities and flaccid paralysis. The artificial squeezing of urine was required twice daily after the rats woke from anesthesia. Due to early unfamiliar surgery and inappropriate medication, 20 rats died, which included 12 rats in the MP group, 5 in the 10 mg muscone group, and 3 in the NS group. A total of 140 adult male SD rats reached clean grade.

Biochemical analysis

Levels of SOD, MDA, TNF-α, IL-1β, and IL-6 as detected by ELISA

The SOD level showed a declining trend in the NS group from 3 hours to 1 week, rising at 2 weeks after traumatic SCI model. The SOD levels in the MP and MO_x groups escalated to the peak from 3 hours to 3 days; these levels were significantly higher than that in the NS group, most obvious in the MO3 group, and declined after 2 weeks. The declining trend was the most obvious in the MO1 group, followed by the MP group, at the same time point. (*Figure 3*, At 3 h and 8 h, P<0.001; 1 day, P<0.003; 3 days and 1 and 2 weeks, P<0.001).

The MDA level in the NS group increased from 3 hours to 1 week and declined after 2 weeks. The level was higher in the MO3 group than in the NS group after 3 and 8 hours, declined after 1 day, escalated to the peak in the MP group after 3 days, and then declined. This trend in the MO1 and MO2 groups was similar to that in the MP group; the level was the lowest in the MO2 group (*Figure 4*, each time point, P<0.001).

The level of TNF-α increased slowly from 3 hours to 1 week and declined after 2 weeks in the NS group. The TNF-α level was lower in the remaining four groups compared with the NS group and was the lowest in the MO2 group; the peak appeared in the MP group after 1 day and then slowly declined. The peak of the TNF-α level appeared in the MO2 group after 8 hours and then declined at the same time points (*Figure 5*).

The level of IL-1β increased slowly from 66.59 to 75.55 ng/L in the NS group from 3 hours to 1 day after a slow decline to 53.75 ng/L in 2 weeks. At the same time, the IL-1β level was lower in the other groups compared with the NS group. The level in the MP group was set to the minimum of 37.34 ng/L after 3 hours. The level in the MO2 group was the lowest after 8 hours, gradually peaked in 1 week, and decreased significantly in 2 weeks. The level in the MO3 group was the maximum, about 62.49 ng/L, in all treatment groups in 1 week (*Figure 6*).

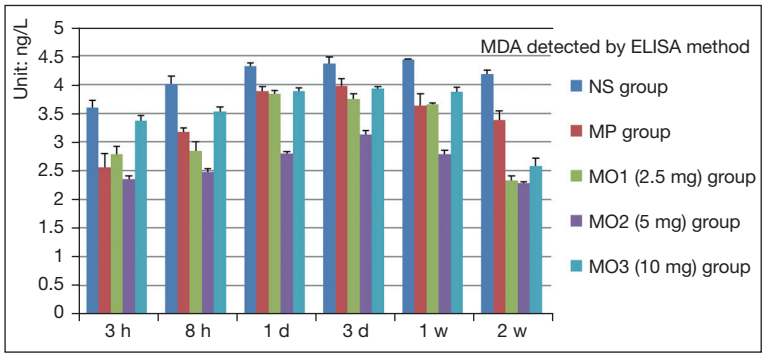

Figure 4 MDA level decreased in the MP and MO_x groups compared with the NS group, with statistically significant differences except in the MO1 and MO2 groups after 2 weeks (F=171.9, P<0.001). In general, the effect in the MO2 group was obvious. MDA, malondialdehyde; MP, methylprednisolone; MO, muscone; NS, normal saline.

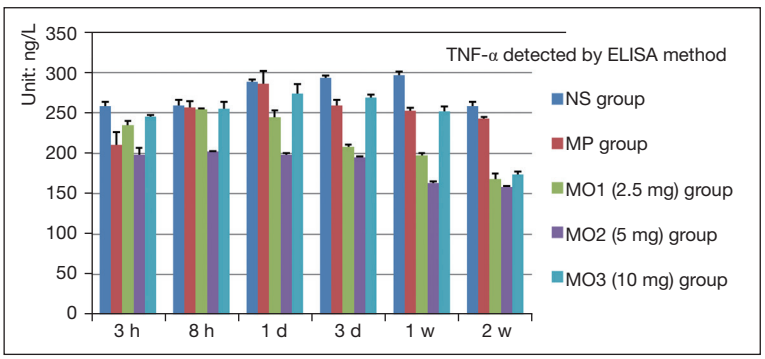

Figure 5 TNF-α level was lower in the MO2 group compared with other groups at all time points (P<0.001). TNF-α, tumor necrosis factor alpha; MO, muscone; NS, normal saline; MP, methylprednisolone.

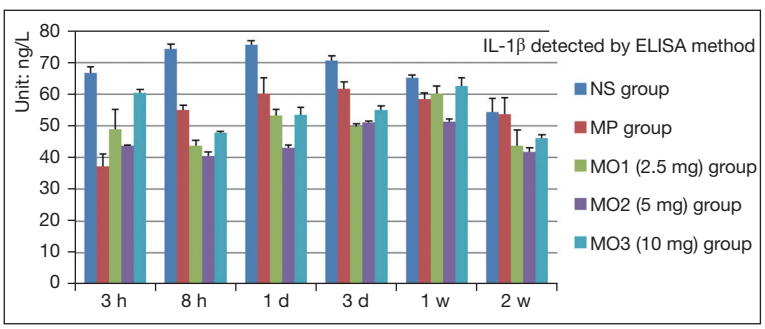

Figure 6 IL-1β level showed a trend similar to that of TNF-α (each point in time, P<0.001). The IL-1β level in the NS group rose slowly from 3 h to 1 day and then declined. The levels in the remaining four groups was lower than that in the NS group. It was the lowest in the MO2 group. The peak appeared in the MP group after 3 days and then slowly declined. The peak appeared in the MO3 group in 8 h and then declined at the same time point. IL-1β, interleukin-1β; TNF-α, tumor necrosis factor alpha; NS, normal saline; MO, muscone; MP, methylprednisolone.

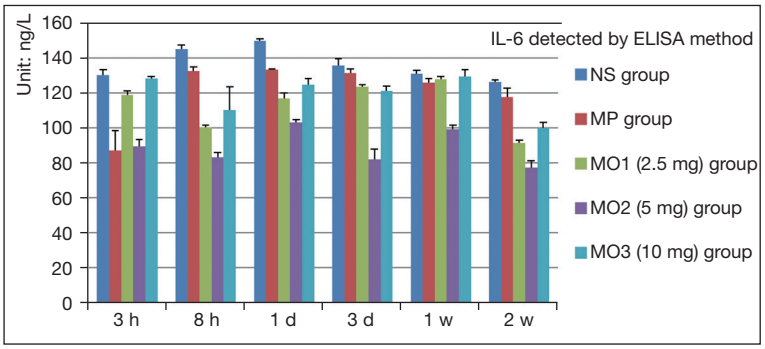

Figure 7 IL-6 level showed a rising trend from 3 h to 1 day after the successful modeling and then slowly decreased. The levels in the MO_x groups were better than those in the NS and MP group, and were more meaningful in the MO2 group. IL-6, interleukin 6; NS, normal saline; MO, muscone; MP, methylprednisolone.

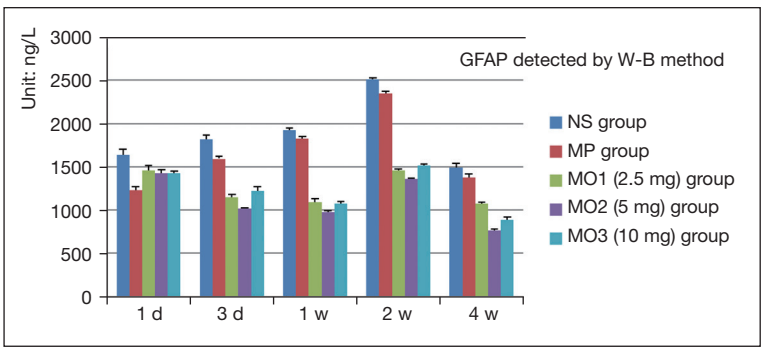

Figure 8 GFAP level increased in the NS and MP groups from 1 day to 2 weeks then declined. Statistically significant differences were found between the NS, MP, and MO_x groups in 3 days, 1 week, 2 weeks, and 4 weeks ($P<0.05$). The level in the MO2 group was the lowest. GFAP, glial fibrillary acidic protein; NS, normal saline; MO, muscone; MP, methylprednisolone.

The level of IL-6 showed a rising trend from 130.27 to 149.61 ng/L in the NS group from 3 hours to 1 day after the successful modeling, and then slowly decreased to 126.15 ng/L in 2 weeks. The levels in the other groups were lower than that in the NS group at the same time point. The level in the MO2 group was the lowest, about 89.16 ng/L, in 3 hours and about 77.29 ng/L in 2 weeks. The MO_x showed the peak in 1 day and 1 week. The peak of the IL-6 level in the MP group was 133.02 ng/L in 1 day and then slowly decreased, reaching 117.63 ng/L in 2 weeks (*Figure 7*).

Levels of glial fibrillary acidic protein (GFAP), B-cell lymphoma-2 (BCL-2), and caspase3 detected by western blot analysis

The levels of GFAP in the NS and MP groups increased from 1 day to 2 weeks and then declined in 4 weeks. The levels in the MO_x groups were equivalent to those in the NS and MP groups after 1 day. The level in the MO2 group was the lowest, 1,013.35 μg/μL, after 3 days. The levels in the NS and MP groups continued to rise. The levels in the MO_x group continued to decline to a minimum of 976.25 μg/μL in 1 week. The levels in the NS and MP groups increased significantly, with the level in the NS group reaching 2513.07 μg/μL and the level in the MP group reaching 2,347.13 μg/μL in 2 weeks. The levels in the MO_x groups showed a slight increase, with the level in the MO2 group still the lowest at 1,356.07 μg/μL. This indicated that GFAP expression in astrocytes was obvious, and the proliferation was the most active in 2 weeks. The level in the NS group was the highest at 1,489.94 μg/μL, while the level in the MO2 group was the lowest at 765.43 μg/μL in 4 weeks (*Figure 8*).

The levels of BCL-2 increased from 1 day to 1 week

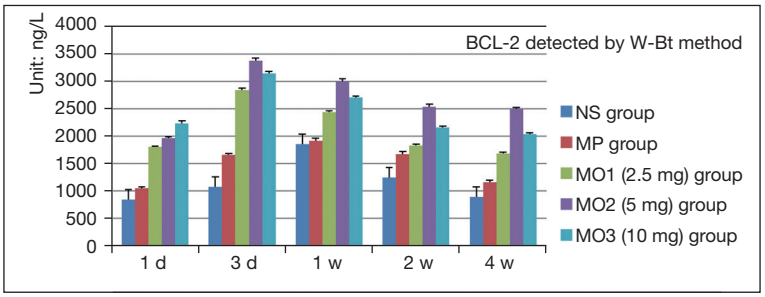

Figure 9 BCL-2 level in the NS group showed a similar trend as in the MP group, rising from 1 day to 1 week and then declining. The level in the MO_x groups was higher and peaked earlier. The level in the MO2 group was remarkable. BCL-2, B-cell lymphoma-2; NS, normal saline; MO, muscone; MP, methylprednisolone.

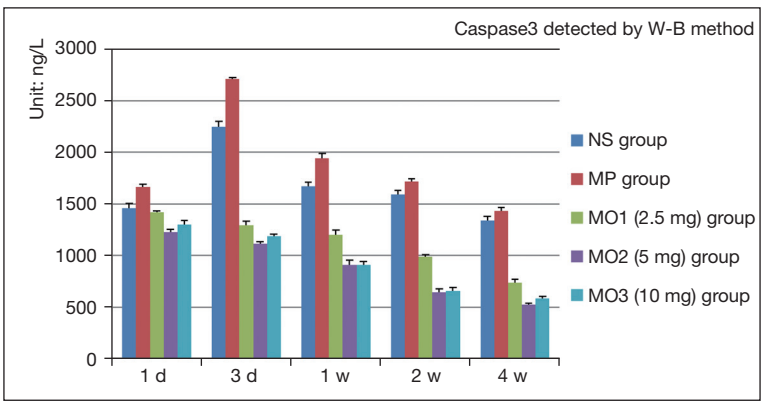

Figure 10 Caspase3 level always decreased in the MO_x groups compared with the NS and MP groups. Statistically significant differences in the levels were found, except in the MO2 and MO3 groups, in 3 days, 1 week, 2 weeks, and 4 weeks ($P<0.05$). NS, normal saline; MO, muscone; MP, methylprednisolone.

and then declined gradually in the NS and MP groups. The BCL-2 levels in the MO_x groups increased from 1 to 3 days and then declined. The level was the lowest in the NS group and the highest in the MO3 group after 1 day. After 3 days, the level in the NS group remained the lowest and the level in the MO3 group was the highest. In 1 week, the levels in the NS and MP groups continued to rise, while those in the MO_x groups showed a decline, being the lowest, 1,857.39 μg/μL, in the NS group and the highest, 2,993.87 μg/μL, in the MO3 group. In 2 weeks, a significant decrease in the levels was noted in all groups, with the lowest in the NS group at 123.31 μg/μL and the highest in the MO3 group at 2,539.77 μg/μL. In 4 weeks, a significant decrease was found in all groups. The level was the lowest in the NS group, at 887.84 μg/μL, and the highest in the MO3 group, at 2,499.47 μg/μL (*Figure 9*).

The level of caspase3 rose from 1 day to 3 days and then declined gradually in the NS and MP groups from 3 days to 4 weeks. The levels in the remaining groups declined from 1 day to 4 weeks. After 1 day, the caspase3 level was the highest in the MP group at 1,663.92 μg/μL and the lowest in the MO2 group at 1,226.19 μg/μL. After 3 days, the level was the highest in the MP group at 2,708.35 μg/μL and the lowest in the MO2 group at 1,113.34 μg/μL. The levels in the remaining groups were between those of the two groups. In 1 week, the level was the highest in the MP group at 1,942.2 μg/μL. In 4 weeks, a significant decrease in the level was found in all groups. The lowest level was in the MO2 group, at 523.68 μg/μL, and the highest was in the MP group, at 1,430.24 μg/μL (*Figure 10*).

Pathological observations

Extensive hemorrhage, cell edema, and pyknosis below the dorsal SCI were observed in 8 hours using HE staining; they were the most obvious in the NS group, followed by

the MP group. The minimal hemorrhage was observed in the MO2 group. A cavity developed between the strike zone and the myelocele. As time progressed, bleeding was less, and pyknosis, necrosis, and cathepsins occurred. The proliferation and activation of astrocytes increased gradually, was significant in 1 week, reached the peak in 2 weeks, and then declined in 4 weeks. In 4 weeks, the cavity enlarged and the myelocele disappeared in the NS group. The scattered small cavities were still observed in the MP group. The cavities were filled with hyperplasia of astrocytes, the cavities in the MO_x groups disappeared, and the inflammatory reaction was the slightest in the MO2 group (*Figure 11*).

After 8 hours, the number of astrocytes increased, as detected by Nissl staining, including obviously enlarged Nissl bodies, fragmentation, maldistribution, and shrunken neurons in the NS group. Nissl bodies were swollen and accumulated, and neurons still shrunk in the MP group. The neurons were more in number and normal in structure, the distribution of Nissl bodies was normal, and the proliferation of astrocytes was less in the MO2 group. With time, a large number of astrocytes appeared, and neuronal pyknosis, karyorrhexis, and the proliferation of astrocytes occurred in the NS group. Some contracted neurons and proliferation of astrocytes were obvious in 4 weeks. At the same time point, the number of neurons in the MO_x groups was high, with structural integrity, but the number of neurons still decreased. Neuronal injury and satellite phenomenon in the MO1, MO3, and MP groups was obvious between the NS group and MO2 group. The spinal cord dorsal horn and injured area showed similar changes (*Figures 12*,*13*).

Immunocytochemistry (ICC) staining revealed hyperplasia of astrocytes in the NS group, reaching the peak at 155.8/vision in 2 weeks and then slowly declining. Hyperplasia of astrocytes was lower in the MP group than in the NS group, peaked at 125.8/vision in 1 week, and then slowly declined. The increase in the number of astrocytes showed a declining trend until 2 weeks and then increased slowly in the MO_x groups. At the same time point, the number of astrocytes was lower in the MO_x groups than in the NS and MP groups. In 4 weeks, a significant decrease was observed in all groups, with the lowest in the MO2 group and the highest in the NS group (*Figure 14*).

Neurological function evaluation after SCI

We recorded BBB scores at six time points, namely, 1, 3, 7, 14, 21, and 28 days. The scores were evaluated in five experimental groups. The changes in the function of lower limbs were not obvious, between 0 grade and 1 grade from 1 to 3 days. With time, the function of lower limbs gradually improved (8.2 in the NS group and 13.6 in the MP group) in 4 weeks. The neurological function was superior in the MO_x groups compared with the MP and NS groups. The recovery was the most obvious in the MO2 group, 10.0 in 2 weeks and 18.6 in 4 weeks (*Figure 15*).

Discussion

SCI is a catastrophic disease associated with loss of nerve function and damaged neurological structures and has become a significant social and economic burden for the health care system and patients' families. The secondary injury following SCI is considered to be due to the continuation of cellular destruction through inflammatory cytokines, which are considered the key regulating substances. Inflammatory cytokines, such as IL-6, IL-1β, and TNF-α, played a very important role during the pathological progression of secondary destructive cascade following primary SCI, exacerbating inflammatory response and leading to further disruption of the blood-spinal cord barrier, which amplified tissue damage and resulted in poor functional recovery (41-45). Yu's research showed that reduced expression of pro-inflammatory cytokines and increased expression of anti-inflammatory factors contributed to a better Basso Mouse Scale (BMS) score (41). The findings were consistent with those of Bethea *et al.* (46), who reported that reduced TNF-α production significantly improved functional recovery following traumatic SCI in rats. Wang (47). reported the increased expression of transforming growth factor (TGF)-β1, TNF-α, IL-1β, and nuclear factor (NF)-κB following the induction of myocardial infarction, and the use of muscone statistically declined the expression of these inflammatory markers. Previous studies have shown that muscone was involved in inhibiting inflammatory reaction (48-51). Our study also demonstrated that the expression of IL-6, IL-1β, and TNF-α increased in all five groups. The inhibitory effect was more obvious in the MO2 group compared with the other four groups, and indicated that the protective effects of muscone might be attributed to its anti-inflammatory effects.

Necrosis and apoptosis also play a key role in SCI. Previous studies have indicated that apoptosis was characterized by the increased expression of pro-apoptotic

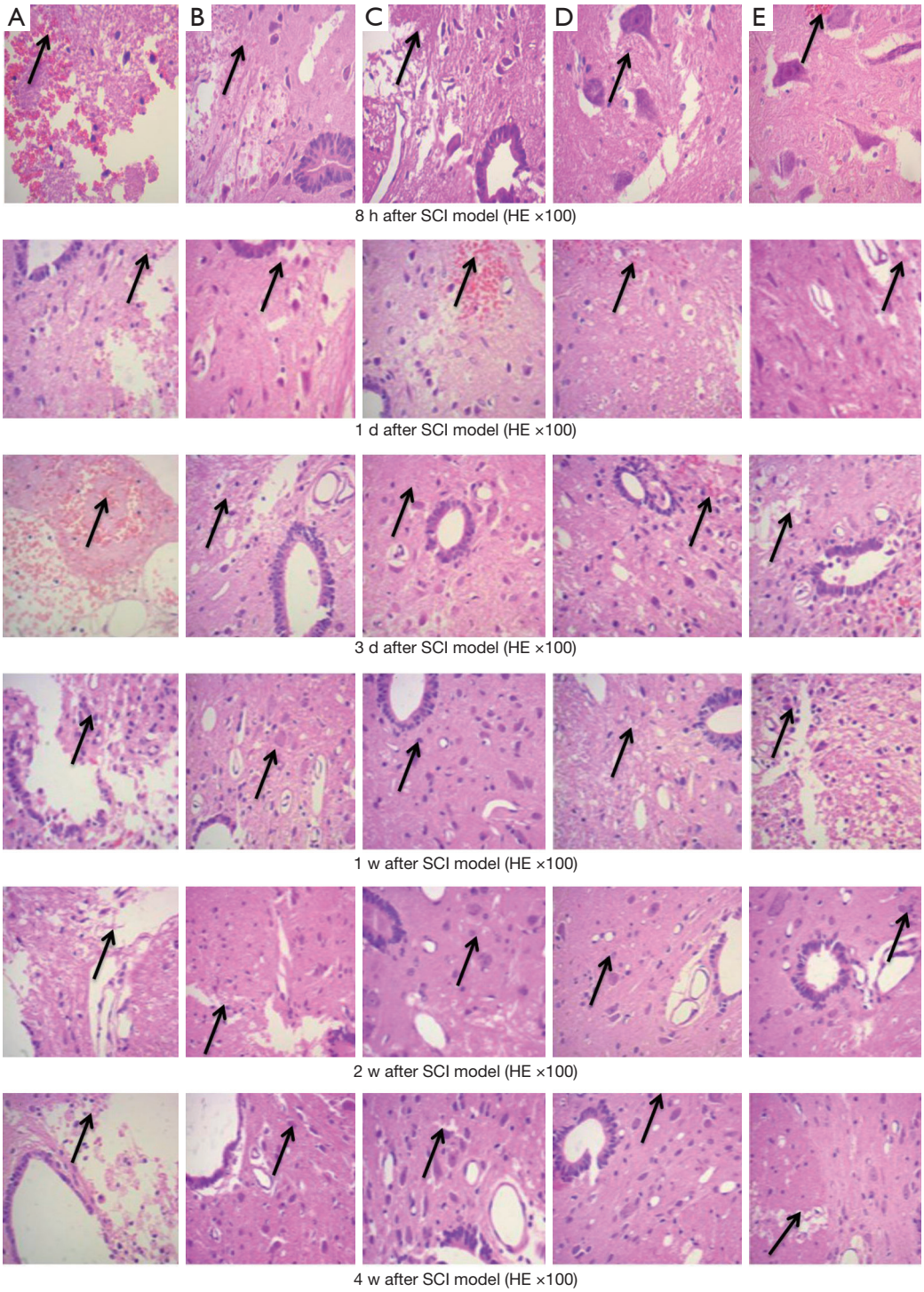

Figure 11 Extensive hemorrhage, cell edema, and pyknosis below the dorsal SCI were observed at 8 hours and 1 day. The proliferation and activation of astrocytes increased gradually and reached the peak at 2 weeks, and then declined at 4 weeks. The cavities were filled with hyperplasia of astrocytes, the cavities in the MO_x groups disappeared, and the inflammatory reaction was the slightest in the MO2 group. Black arrows mark extensive hemorrhage at 8 hour and 1 day after SCI model. Black arrows mark cavities after SCI model. Black arrows mark proliferation and activation of astrocytes at 1 week and 2 weeks after SCI model. Arrows mark proliferation and activation of astrocytes at 4 weeks after SCI. SCI by HE staining. SCI, spinal cord injury; HE, hematoxylin-eosin; MO, muscone.

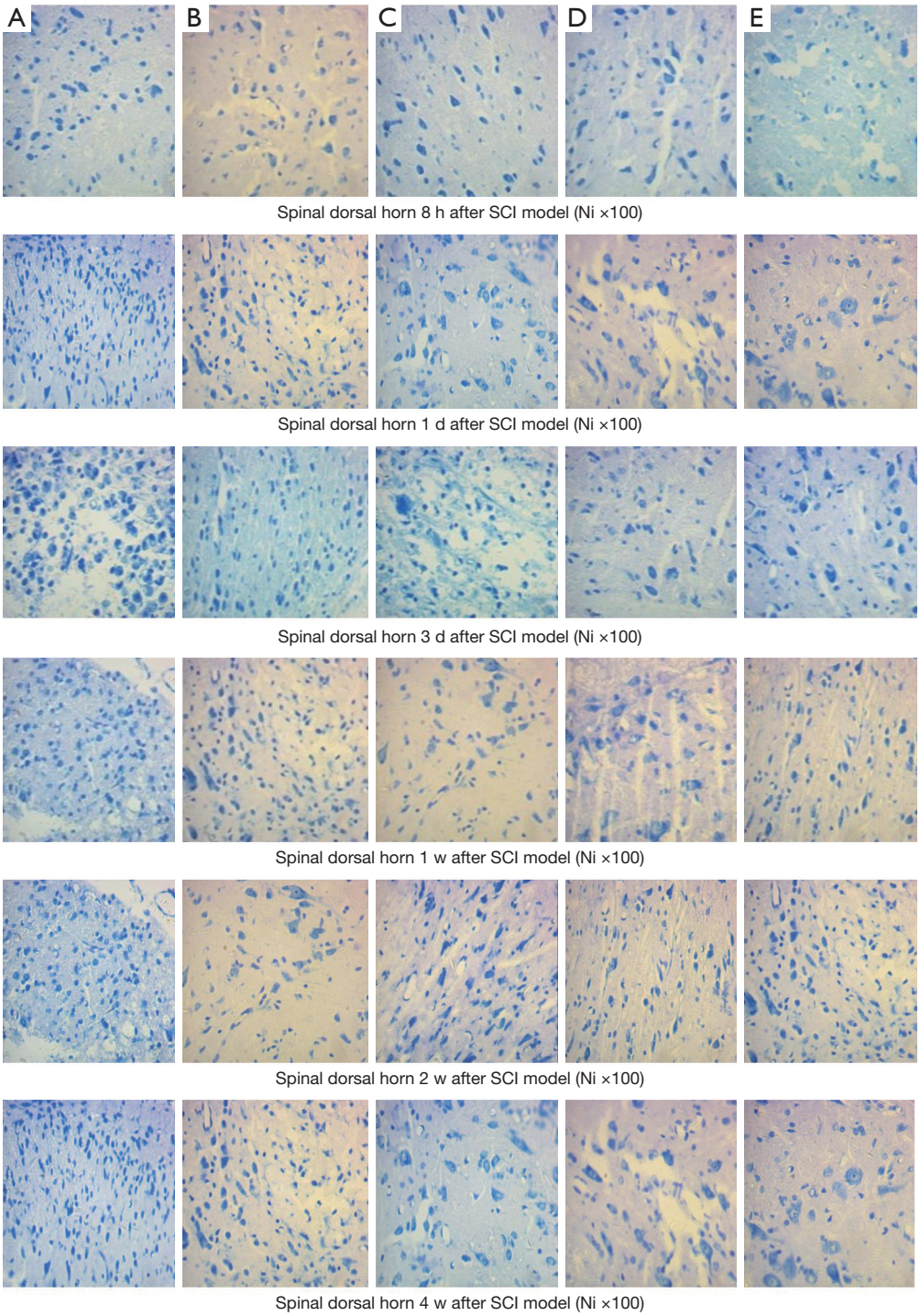

Figure 12 The number of astrocytes increased, as detected by Nissl staining in the NS group and MP group at different time points. Some contracted neurons and proliferation of astrocytes were obvious in 4 weeks. The proliferation of astrocytes was less in the MO2 group than other groups at different time points. Neuronal injury and satellite phenomenon in the MO1, MO3, and MP groups was obvious between the NS group and MO2 group in 4 weeks. Spinal dorsal horn after SCI by Nissl staining; NS, normal saline; MO, muscone; MP, methylprednisolone; SCI, spinal cord injury.

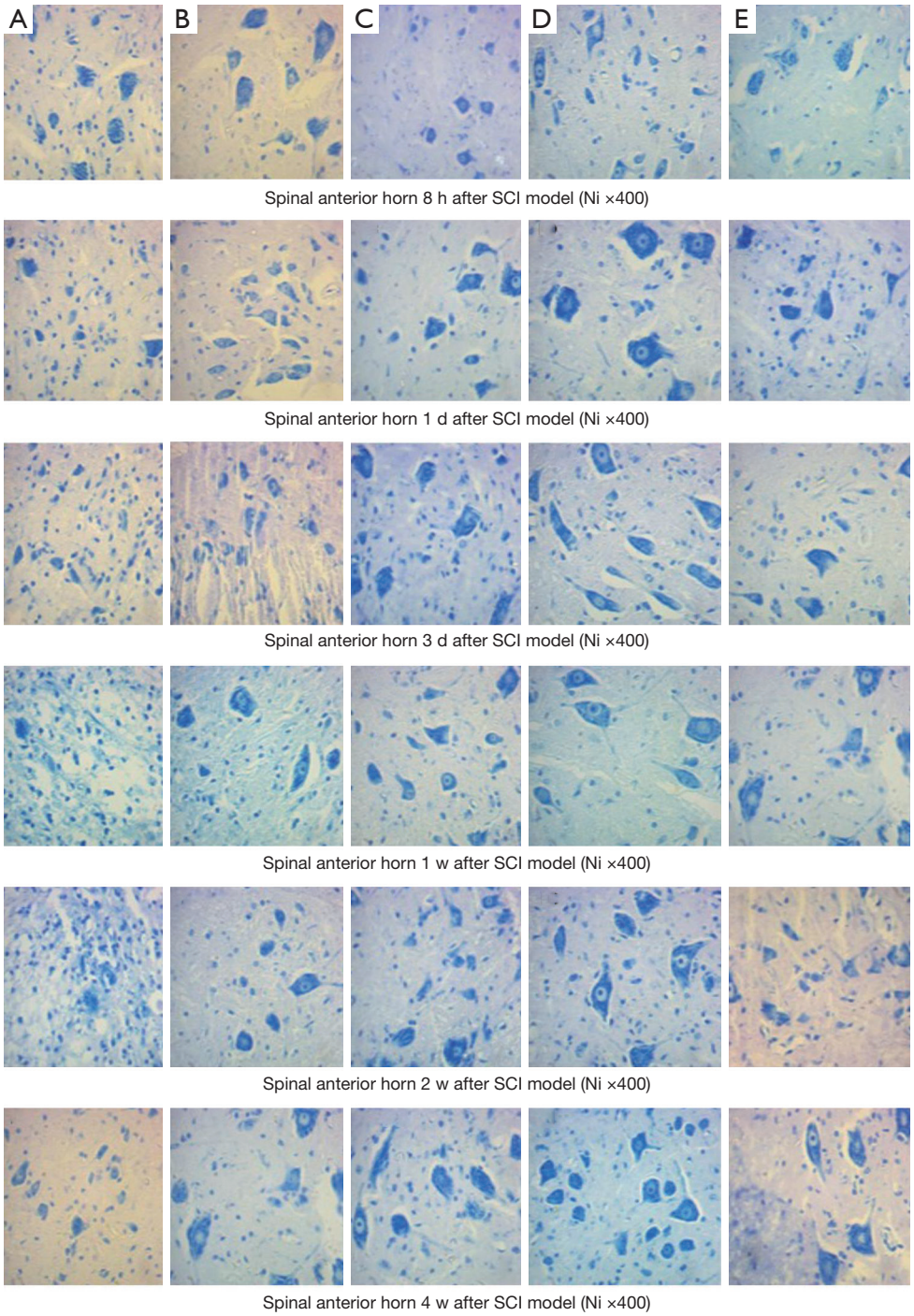

Figure 13 The number of astrocytes increased, as detected by Nissl staining, shrunken neurons in the NS group and MP group at different time points. Some contracted neurons and proliferation of astrocytes were obvious in 4 weeks. At the same time point, the number of neurons in the MO_x groups was high, with structural integrity. The neurons were more in number and normal in structure, and the proliferation of astrocytes was less in the MO2 group. Spinal dorsal horn after SCI by Nissl staining; NS, normal saline; MO, muscone; MP, methylprednisolone; SCI, spinal cord injury.

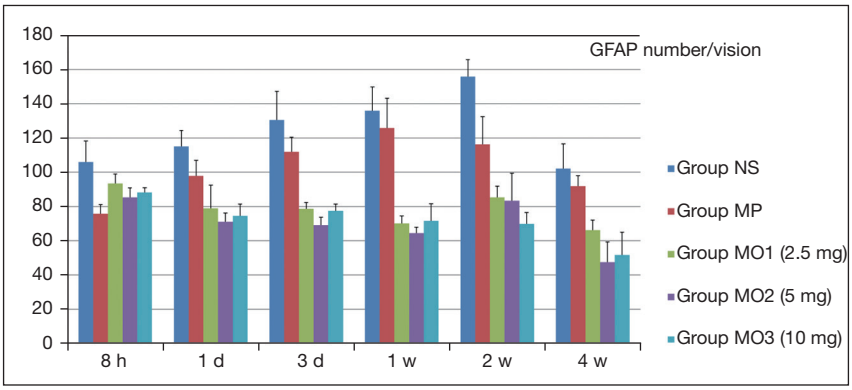

Figure 14 Statistically significant differences in the number of astrocytes between the MP, NS, and MO_x groups at all time points (P<0.05). The number was the lowest in the MO2 group. GFAP, glial fibrillary acidic protein; NS, normal saline; MO, muscone; MP, methylprednisolone.

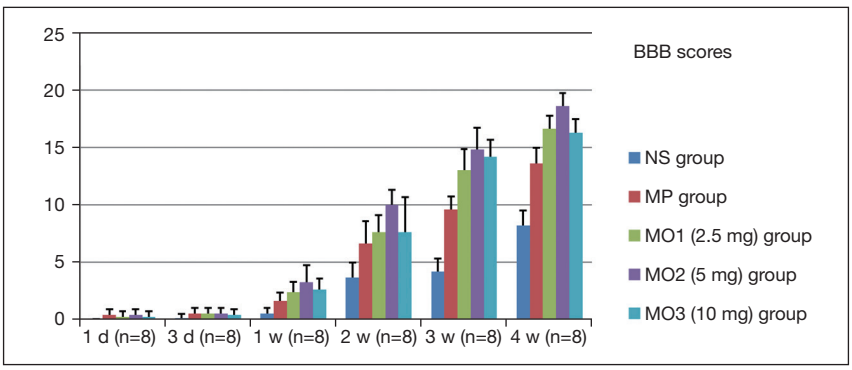

Figure 15 The changes in the function of lower limbs were not obvious, between 0 grade and 1 grade from 1 day to 3 days (P>0.05). Neurological function was superior in the MO_x group compared with the MP and NS groups from 1 to 4 weeks (P<0.05). It was the most obvious in the MO2 group, 10.0 in 2 weeks and 18.6 in 4 weeks. All groups showed significant differences in 3 and 4 weeks (P<0.05). BBB, Basso-Beattie-Bresnahan; NS, normal saline; MO, muscone; MP, methylprednisolone.

BCL2-associated X (Bax) family proteins and the decreased expression of anti-apoptotic Bcl-2 family proteins (52-55). The caspase cascade also plays an important role in apoptosis. Caspase3 typically functions downstream of other caspases and directly activates enzymes responsible for DNA fragmentation in the intrinsic apoptotic pathway (56,57). A loss of ionic homeostasis is observed. The phagocytic inflammatory cells release reactive oxygen species, upregulating the release of excitatory amino acids and inflammatory cytokines and thus inducing apoptosis. Wei elucidated that muscone exerted neuroprotective effects *in vivo* and *in vitro* (58).

Apoptosis is known as a naturally occurring physiological process and may play a key role in secondary SCI. The long-term neurological deficits following SCI might result from a large range of apoptosis of neurons and oligodendrocytes in the injured spinal cord, so a better understanding of apoptosis following SCI will lead to novel strategies for therapeutic interventions. Injury-induced apoptosis could be observed in neurons, astrocytes, oligodendroglia and microglia in rat SCI (59). The aim of treatment of SCI is to reduce secondary neuronal damage (60), upregulate the release of anti-inflammatory cytokines, reduce oxidative stress to enhance neural cell survival in preclinical models of traumatic SCI (61), and Inhibit hyperplasia of astrocytes and scar formation. There are many treatments for spinal cord injury, including medications, cell transplantation, exosomes, tissue engineering, cell reprogramming, and rehabilitation (62). As an important branch of worldwide medical research, traditional Chinese medicine (TCM) is rapidly moving

towards a path of reform and innovation. 16 active ingredients, nine herbs, and three compound prescriptions were used for treatment of spinal cord injury (63).

In our study, the results revealed that an increase in the levels of Bcl-2 family proteins and a decrease in the level of caspase3, increased SOD production, and decreased MDA production were more remarkable in the MO2 group compared with the other groups. Thus, we considered that muscone played a protective role due to its anti-apoptotic effects.

Regeneration is often hindered by the presence of a substantial postinjury cystic cavity, glial cell hyperplasia, and glial scar formation, which lacks the substrate to support cell migration and axon growth (2,64,65). The excitatory amino acids such as glutamate and aspartate are released under the action of the immune-inflammatory response, and the secretion of inflammatory cytokines increases. The activation of a large number of astrocytes, leading to hyperplasia and hypertrophy of astrocytes, in the early stage of injury has a certain protective effect on the expansion of damage, but the activation of a large number of astrocytes in a late stage, forming collagen fibers and scars, prevents the growth of nerves and causes spinal cord function disorder (58). In our study, HE, Nissl, and GFAP staining indicated astrocyte proliferation. The changes were most obvious in the NS group, with necrosis, expansion of the cavity, disappearance of the neuronal structure, and hyperplasia of astrocytes, followed by the MP group. The pathological changes in the spinal cord treated with the three doses of muscone were mild, with the least damage in the MO2 group (5 mg/kg). The results indicated that the inflammatory responses were suppressed, and neuronal necrosis and apoptosis were also inhibited. In addition, cystic cavities and hyperplasia of astrocytes were controlled. The expression of the GFAP protein was lower than that in the NS and MP groups. Moreover, our study showed that the lower limb recovery was better in the MO_x groups than in the NS and MP groups according to BBB scores (66,67); the recovery was remarkable in the MO2 group. Our results reflected the positive role of muscone in neuroregeneration, leading to better functional recovery following SCI. However, MPSS had no obvious effect on apoptosis and the correction of neurotic function (68).

This study was the first to demonstrate the protective effects of muscone against traumatic SCI. The experiment data found that different concentrations of muscone played a positive role by inhibiting immune-inflammatory reaction, downregulating the expression of caspase3, upregulating the expression of BCL-2, reducing necrosis and apoptosis of neurons and astrocytes, lowering the expression of GFAP, inhibiting the excessive proliferation of astrocytes, and improving the function of lower limbs after traumatic SCI in rats. The effect of 5 mg/kg dose muscone was remarkable and better than that of MPSS.

Conclusions

This study was novel in showing that muscone alleviated secondary injury after SCI by reducing inflammation and anti-apoptotic effect and provided favorable conditions for neuroregeneration in rats. Therefore, we believe that muscone may serve as a promising and effective drug for traumatic SCI treatment.

There are also some limitations in this study, including the potential bias from the small number of samples in each group and the inconsistency of smoothness and proficiency in blood collection. When traumatic SCI models were stablished, there may be accidental injury of spinal cord due to surgical operation. There is no complete standardization when striking. It may also cause inaccuracies related to the results.

Acknowledgments

Funding: This work was supported by Chongqing Science and Technology Bureau (Project No. cstc2016jcyja0299).

Footnote

Reporting Checklist: The authors have completed the ARRIVE reporting checklist Available at https://atm.amegroups.com/article/view/10.21037/atm-22-2672/rc

Data Sharing Statement: Available at https://atm.amegroups.com/article/view/10.21037/atm-22-2672/dss

Conflicts of Interest: All authors have completed the ICMJE uniform disclosure form (available at https://atm.amegroups.com/article/view/10.21037/atm-22-2672/coif). The authors have no conflicts of interest to declare.

Ethical Statement: The authors are accountable for all aspects of the work in ensuring that questions related to the accuracy or integrity of any part of the work are appropriately investigated and resolved. Experiments were performed under a project license granted by the

Ethics Review Board of the University-Town Hospital of Chongqing Medical University (No. LL-202133), in compliance with national guidelines for the care and use of animals.

References

1. Eckert MJ, Martin MJ. Trauma: Spinal Cord Injury. Surg Clin North Am 2017;97:1031-45.
2. Eli I, Lerner DP, Ghogawala Z. Acute Traumatic Spinal Cord Injury. Neurol Clin 2021;39:471-88.
3. Galeiras Vázquez R, Ferreiro Velasco ME, Mourelo Fariña M, et al. Update on traumatic acute spinal cord injury. Part 1. Med Intensiva 2017;41:237-47.
4. Mourelo Fariña M, Salvador de la Barrera S, Montoto Marqués A, et al. Update on traumatic acute spinal cord injury. Part 2. Med Intensiva 2017;41:306-15.
5. Tator CH. Update on the pathophysiology and pathology of acute spinal cord injury. Brain Pathol 1995;5:407-13.
6. Hayta E, Elden H. Acute spinal cord injury: A review of pathophysiology and potential of non-steroidal anti-inflammatory drugs for pharmacological intervention. J Chem Neuroanat 2018;87:25-31.
7. Afferi L, Pannek J, Louis Burnett A, et al. Performance and safety of treatment options for erectile dysfunction in patients with spinal cord injury: A review of the literature. Andrology 2020;8:1660-73.
8. Bourguignon L, Vo AK, Tong B, et al. Natural Progression of Routine Laboratory Markers after Spinal Trauma: A Longitudinal, Multi-Cohort Study. J Neurotrauma 2021;38:2151-61.
9. Norenberg MD, Smith J, Marcillo A. The pathology of human spinal cord injury: defining the problems. J Neurotrauma 2004;21:429-40.
10. Alizadeh A, Dyck SM, Karimi-Abdolrezaee S. Traumatic Spinal Cord Injury: An Overview of Pathophysiology, Models and Acute Injury Mechanisms. Front Neurol 2019;10:282.
11. Keane RW, Kraydieh S, Lotocki G, et al. Apoptotic and anti-apoptotic mechanisms following spinal cord injury. J Neuropathol Exp Neurol 2001;60:422-9.
12. Rabinstein AA. Traumatic Spinal Cord Injury. Continuum (Minneap Minn) 2018;24:551-66.
13. David S, López-Vales R, Wee Yong V. Harmful and beneficial effects of inflammation after spinal cord injury: potential therapeutic implications. Handb Clin Neurol 2012;109:485-502.
14. Beattie MS, Farooqui AA, Bresnahan JC. Review of current evidence for apoptosis after spinal cord injury. J Neurotrauma 2000;17:915-25.
15. Vargova I, Machova Urdzikova L, Karova K, et al. Involvement of mTOR Pathways in Recovery from Spinal Cord Injury by Modulation of Autophagy and Immune Response. Biomedicines 2021;9:593.
16. Liu M, Wu W, Li H, et al. Necroptosis, a novel type of programmed cell death, contributes to early neural cells damage after spinal cord injury in adult mice. J Spinal Cord Med 2015;38:745-53.
17. Cao L, Mu W. Necrostatin-1 and necroptosis inhibition: Pathophysiology and therapeutic implications. Pharmacol Res 2021;163:105297.
18. Nakamura M, Houghtling RA, MacArthur L, et al. Differences in cytokine gene expression profile between acute and secondary injury in adult rat spinal cord. Exp Neurol 2003;184:313-25.
19. Firat T, Kukner A, Ayturk N, et al. The Potential Therapeutic Effects of Agmatine, Methylprednisolone, and Rapamycin on Experimental Spinal Cord Injury. Cell J 2021;23:701-7.
20. Ahmed L, Zhang Y, Block E, et al. Molecular mechanism of activation of human musk receptors OR5AN1 and OR1A1 by (R)-muscone and diverse other musk-smelling compounds. Proc Natl Acad Sci U S A 2018;115:E3950-8.
21. Chen ZZ, Du SY, Lu Y, et al. Mechanism research of aromatics borneol and muscone. Journal of Chinese Medicinal Materials 2014;37:460-4.
22. Meng Y, Xiao Q, Bai JY, et al. Resolution and chiral recognition of muscone as well as actions on neural system. J Asian Nat Prod Res 2014;16:1166-70.
23. Wang N, Chang GJ, Jin QZ, et al. Analysis of muscone from serum and cerebrospinal fluid of rabbits after intragastric administration of tongqiao huoxue granules. Journal of Chinese Medicinal Materials 2012;35:1291-4.
24. Chen WK, Huang YF, Wang HD. An experimental study on distribution of musk into the brain through blood brain barrier. Journal of Chinese Integrative Medicine

2004;2:288-91.
25. Chen Z, Gong X, Lu Y, et al. Enhancing effect of borneol and muscone on geniposide transport across the human nasal epithelial cell monolayer. PLoS One 2014;9:e101414.
26. Wang GY, Wang N, Liao HN. Effects of Muscone on the Expression of P-gp, MMP-9 on Blood-Brain Barrier Model In Vitro. Cell Mol Neurobiol 2015;35:1105-15.
27. Yu L, Wang N, Zhang Y, et al. Neuroprotective effect of muscone on glutamate-induced apoptosis in PC12 cells via antioxidant and Ca(2+) antagonism. Neurochem Int 2014;70:10-21.
28. Du Y, Ge Y, Xu Z, et al. Hypoxia-Inducible Factor 1 alpha (HIF-1α)/Vascular Endothelial Growth Factor (VEGF) Pathway Participates in Angiogenesis of Myocardial Infarction in Muscone-Treated Mice: Preliminary Study. Med Sci Monit 2018;24:8870-7.
29. He MC, Shi Z, Qin M, et al. Muscone Ameliorates LPS-Induced Depressive-Like Behaviors and Inhibits Neuroinflammation in Prefrontal Cortex of Mice. Am J Chin Med 2020;48:559-77.
30. Ge JB, Fan WH, Zhou JM, et al. Efficacy and safety of Shexiang Baoxin pill (MUSKARDIA) in patients with stable coronary artery disease: a multicenter, double-blind, placebo-controlled phase IV randomized clinical trial. Chin Med J (Engl) 2020;134:185-92.
31. Du Y, Gu X, Meng H, et al. Muscone improves cardiac function in mice after myocardial infarction by alleviating cardiac macrophage-mediated chronic inflammation through inhibition of NF-κB and NLRP3 inflammasome. Am J Transl Res 2018;10:4235-46.
32. Dong J, Li H, Bai Y, et al. Muscone ameliorates diabetic peripheral neuropathy through activating AKT/mTOR signalling pathway. J Pharm Pharmacol 2019;71:1706-13.
33. Yu S, Zhao G, Han F, et al. Muscone relieves inflammatory pain by inhibiting microglial activation-mediated inflammatory response via abrogation of the NOX4/JAK2-STAT3 pathway and NLRP3 inflammasome. Int Immunopharmacol 2020. [Epub ahead of print].
34. Cen W, Chen Z, Gu N, et al. Prevention of AMI induced ventricular remodeling: Inhibitory effect of heart-protecting musk pill on IL-6 and TNF-α. Evid Based Complement Alternat Med 2017. doi: 10.1155/2017/3217395.
35. Feng Q, Liu J. Progress on pharmacological activity of muscone. Food and Drug 2015;17:212-4.
36. Wang M, Shan Y, Sun W, et al. Effects of Shexiang Baoxin Pill for Coronary Microvascular Function: A Systematic Review and Meta-Analysis. Front Pharmacol 2021;12:751050.
37. Kailiang Z, Yihui Z, Dingsheng L, et al. Effects of Muscone on Random Skin Flap Survival in Rats. J Reconstr Microsurg 2016;32:200-7.
38. Li L, Wang N, Jin Q, et al. Protection of Tong-Qiao-Huo-Xue Decoction against Cerebral Ischemic Injury through Reduction Blood-Brain Barrier Permeability. Chem Pharm Bull (Tokyo) 2017;65:1004-10.
39. Chen Z. Pien Tze Huang (PZH) as a Multifunction Medicinal Agent in Traditional Chinese Medicine (TCM): a review on cellular, molecular and physiological mechanisms. Cancer Cell Int 2021;21:146.
40. Api AM, Gudi R. An in vivo mouse micronucleus assay on musk ketone. Mutat Res 2000;464:263-7.
41. Yu WR, Fehlings MG. Fas/FasL-mediated apoptosis and inflammation are key features of acute human spinal cord injury: implications for translational, clinical application. Acta Neuropathol 2011;122:747-61.
42. Rolls A, Shechter R, Schwartz M. The bright side of the glial scar in CNS repair. Nat Rev Neurosci 2009;10:235-41.
43. Wang XJ, Peng CH, Zhang S, et al. Polysialic-Acid-Based Micelles Promote Neural Regeneration in Spinal Cord Injury Therapy. Nano Lett 2019;19:829-38.
44. Hellenbrand DJ, Quinn CM, Piper ZJ, et al. Inflammation after spinal cord injury: a review of the critical timeline of signaling cues and cellular infiltration. J Neuroinflammation 2021;18:284.
45. Cunha MI, Su M, Cantuti-Castelvetri L, et al. Pro-inflammatory activation following demyelination is required for myelin clearance and oligodendrogenesis. J Exp Med 2020;217:e20191390.
46. Bethea JR, Nagashima H, Acosta MC, et al. Systemically administered interleukin-10 reduces tumor necrosis factor-alpha production and significantly improves functional recovery following traumatic spinal cord injury in rats. J Neurotrauma 1999;16:851-63.
47. Wang X, Meng H, Chen P, et al. Beneficial effects of muscone on cardiac remodeling in a mouse model of myocardial infarction. Int J Mol Med 2014;34:103-11.
48. Belsito D, Bickers D, Bruze M, et al. A toxicological and dermatological assessment of macrocyclic ketones when used as fragrance ingredients: the RIFM Expert Panel. Food Chem Toxicol 2011;49 Suppl 2:S126-41.
49. Jiang B, Cai F, Gao S, et al. Induction of cytochrome P450 3A by Shexiang Baoxin Pill and its main components. Chem Biol Interact 2012;195:105-13.
50. Chen ZZ, Lu Y, Du SY, et al. Influence of borneol and muscone on geniposide transport through MDCK and

MDCK-MDR1 cells as blood-brain barrier in vitro model. Int J Pharm 2013;456:73-9.
51. Liu P, Feng Y, Dong C, et al. Administration of BMSCs with muscone in rats with gentamicin-induced AKI improves their therapeutic efficacy. PLoS One 2014;9:e97123.
52. Rohde LE, Ducharme A, Arroyo LH, et al. Matrix metalloproteinase inhibition attenuates early left ventricular enlargement after experimental myocardial infarction in mice. Circulation 1999;99:3063-70.
53. Kluck RM, Bossy-Wetzel E, Green DR, et al. The release of cytochrome c from mitochondria: a primary site for Bcl-2 regulation of apoptosis. Science 1997;275:1132-6.
54. Yang J, Liu X, Bhalla K, et al. Prevention of apoptosis by Bcl-2: release of cytochrome c from mitochondria blocked. Science 1997;275:1129-32.
55. Tamm I, Schriever F, Dörken B. Apoptosis: implications of basic research for clinical oncology. Lancet Oncol 2001;2:33-42.
56. Oubrahim H, Stadtman ER, Chock PB. Mitochondria play no roles in Mn(II)-induced apoptosis in HeLa cells. Proc Natl Acad Sci U S A 2001;98:9505-10.
57. Lakhani SA, Masud A, Kuida K, et al. Caspases 3 and 7: key mediators of mitochondrial events of apoptosis. Science 2006;311:847-51.
58. Wei G, Chen DF, Lai XP, et al. Muscone exerts neuroprotection in an experimental model of stroke via inhibition of the fas pathway. Nat Prod Commun 2012;7:1069-74.
59. Shi Z, Yuan S, Shi L, et al. Programmed cell death in spinal cord injury pathogenesis and therapy. Cell Prolif 2021;54:e12992.
60. Han B, Liang W, Hai Y, et al. Elucidating the Potential Mechanisms Underlying Distraction Spinal Cord Injury-Associated Neuroinflammation and Apoptosis. Front Cell Dev Biol 2022;10:839313.
61. Anjum A, Yazid MD, Fauzi Daud M, et al. Spinal Cord Injury: Pathophysiology, Multimolecular Interactions, and Underlying Recovery Mechanisms. Int J Mol Sci 2020;21:7533.
62. Fan B, Wei Z, Feng S. Progression in translational research on spinal cord injury based on microenvironment imbalance. Bone Res 2022;10:35.
63. Lu Y, Yang J, Wang X, et al. Research progress in use of traditional Chinese medicine for treatment of spinal cord injury. Biomed Pharmacother 2020;127:110136.
64. Donovan J, Kirshblum S. Clinical Trials in Traumatic Spinal Cord Injury. Neurotherapeutics 2018;15:654-68.
65. Rodríguez-Barrera R, Rivas-González M, García-Sánchez J, et al. Neurogenesis after Spinal Cord Injury: State of the Art. Cells 2021;10:1499.
66. Basso DM, Beattie MS, Bresnahan JC. A sensitive and reliable locomotor rating scale for open field testing in rats. J Neurotrauma 1995;12:1-21.
67. Basso DM, Beattie MS, Bresnahan JC, et al. MASCIS evaluation of open field locomotor scores: effects of experience and teamwork on reliability. Multicenter Animal Spinal Cord Injury Study. J Neurotrauma 1996;13:343-59.
68. Pereira JE, Costa LM, Cabrita AM, et al. Methylprednisolone fails to improve functional and histological outcome following spinal cord injury in rats. Exp Neurol 2009;220:71-81.

Cite this article as: Yu C, Gui F, Huang Q, Luo Y, Zeng Z, Li R, Guo L. Protective effects of muscone on traumatic spinal cord injury in rats. Ann Transl Med 2022;10(12):685. doi: 10.21037/atm-22-2672

